

USE OF FACTS TYPE SVC DEVICES IN HIGH-VOLTAGE ELECTRIC POWER TRANSMISSION SYSTEMS IN ORDER TO INCREASE DYNAMIC STABILITY IN THE PRESENCE OF RENEWABLE ENERGY SOURCES

Andrei COTEANU¹, Ștefan GHEORGHE², Lucian TOMA³

This paper aims to analyse the challenges faced by high-voltage electric power transmission systems in the presence of renewable energy generation sources in terms of dynamic stability. To increase the capacity to integrate renewables into the grid and accelerate the transition from traditional energy sources with an environmental impact to green energy sources, the use of modern technologies such as FACTS is necessary. In this paper, the opportunity to use SVC devices to improve the functioning of the network was analysed. For the dynamic regime simulations, a standardized test network, NORDIC32, was used. This paper concludes that the integration of renewables is feasible and necessary, but it must be accompanied by a reformulation of control strategies of the power system.

Keywords: Dynamic stability of electric power transmission systems, integration of renewable energy sources, FACTS technologies, SVC (Static VAr Compensator), NORDIC32.

1. Introduction

The main challenge currently faced by power systems is the transition from classic, centralized generation, characterized by high and very high-power plants, to distributed generation, which involves units of lower power, evenly distributed at the grid level, being positioned closer to consumers. Complementary to the change in the vision on the distribution of energy sources in the grid, the current trend is to transition from conventional power plants to plants based on renewable energy sources (wind, photovoltaic, biomass, micro-hydropower plants etc.). In addition, the way consumers interact with the network is also changing, if in the past they had only a passive role, they become more actively involved in the functioning of the system by assuming the role of prosumer. Although it brings

¹ PhD Student, Eng Dept. of Electrical Power Systems, National University of Science and Technology POLITEHNICA Bucharest, Romania, e-mail: andrei.coteanu@ed-c.ro

² Prof., Dept. of Electrical Power Systems, National University of Science and Technology POLITEHNICA Bucharest, Romania, e-mail: stefan.gheorghe2506@upb.ro

³ Prof., Dept. of Electrical Power Systems, National University of Science and Technology POLITEHNICA Bucharest, Romania, e-mail: lucian.toma@upb.ro

new challenges, the transition to low-environmental energy sources is urgently needed to ensure decrease on the level of pollution. It is necessary to assess the impact of all these transition processes both from the point of view of static functioning regimes and from the point of view of dynamic regimes. All these challenges need tailor-made technical solutions that help energy systems function properly in a constantly changing environment. A possible solution to increase the dynamic stability of electricity transmission networks in the presence of renewable energy sources are the FACTS SVC – Static VAR Compensator devices [1]. They offer a wide range of benefits and can be used in electricity transmission and distribution systems to increase system stability, regulate voltage levels, reduce energy losses and control power circulation [2]. In the process of determining the optimal response solutions for all these challenges, it is necessary to use standardized test networks and specialized test software solutions [3]. Standardized test networks help assess the impact and model response scenarios for multiple operating scenarios. By using test networks, the operating regimes for several transition situations can be compared, starting from the basic regime in which the energy sources are conventional (hydropower, coal-fired power plant, nuclear power plants) to regimes in which the main energy source in a certain area of the network is renewable [4]. The primary objective of the analysis presented in this article is to determine the impact of large-scale integration of renewable energy sources, specifically wind power plants, into a regional area of an electric power network on the system's dynamic stability. To enhance the dynamic stability of the system in the presence of renewable energy sources, the study further investigates the applicability and effectiveness of FACTS-type devices, namely Static VAR Compensators (SVCs). An analysis of the benefits obtained by using SVC devices in the network was performed through steady state and dynamic mode simulations in the NORDIC32 network. The NORDIC32 network was selected for the present study, as it represents a well-established test system that is widely accepted and employed in CIGRE and IEEE studies. NEPLAN 10 simulation software was used for steady-state calculations and dynamic analysis of the power network. Using this computational tool, simulations of system operation under the investigated scenarios were carried out.

The main objective of the analysis presented in this paper is to examine the behaviour of a transmission power system in the presence of large-scale integration of renewable energy sources. Under this transition scenario toward renewable-based generation, the stability of a selected area of the transmission network was investigated for various operating conditions.

The specific objectives of this analysis include: selecting an appropriate test network for simulation purposes; defining the analysed scenarios to ensure accurate and realistic results; evaluating the results obtained for all studied scenarios and

operating conditions; and determining appropriate measures to address the deficiencies identified during the transition toward renewable energy sources.

2. Static reactive power compensator

2.1. The generic one-line diagram

A definition accepted by international professional organizations in the energy field for VAR compensators is: static VAR compensators are static generators of reactive power in which the change of the capacitive or inductive current results in a change in the output quantities that allows the control or maintenance of certain parameters of the electrical power system, generally the voltage in a grid node [5].

SVCs (Static VAR Compensator) are equipment that connects in the shunt, consisting of coils and capacitors statically controlled with the help of thyristors [6]. The simplified scheme of operation of an SVC device is shown in Fig. 1.

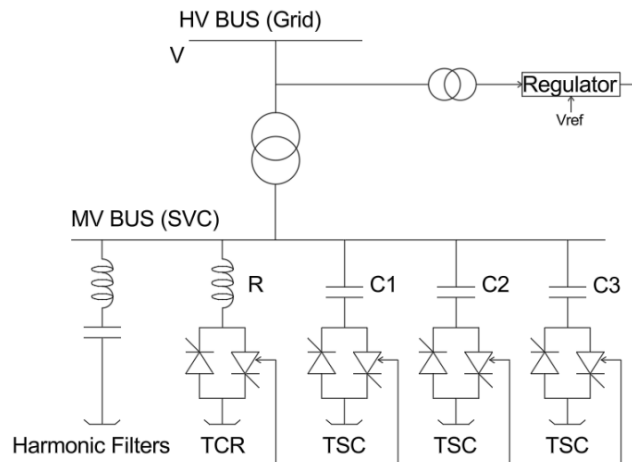


Fig. 1. Schematic diagram of an SVC device [5]

The use of static VAR compensators can increase the performance of the electrical systems in which they are installed. Among the advantages of using SVCs in transmission grids, the most important are [7]:

- damping of voltage and power fluctuations in the network;
- contributes to reducing power losses on transmission lines;
- stabilizes the voltage level in the system;
- contribute to increasing the transmission capacity of power lines;
- improves the stability of the system.

The operation of the static reactive power compensator is based on compensating for variations in the reactive power of consumers using a coil and a capacitor bank [8]. The continuous regulation of the current is carried out with the

help of the coil (TCR), and by means of the capacitor bank (TSC) the balance of the reactive power absorbed by the load and compensator assembly is corrected [9].

2.2. Simplified SVC model for steady-state calculations

In steady state, the SVC is modelled as a controlled susceptance. The reactor impedance is given by $\underline{Z}_L \approx jX_L(\alpha)$, with $X_L(\alpha) > 0$, and the capacitive impedance is $\underline{Z}_C \approx jX_C$, with $X_C < 0$ [135]. Since the reactor and the capacitors are connected in parallel, the equivalent impedance of the SVC is [7]:

$$\underline{Z}_e = \frac{\underline{Z}_L \underline{Z}_C}{\underline{Z}_L + \underline{Z}_C} \cong -\frac{X_L(\alpha)X_C}{j(X_L(\alpha)+X_C)} = j\frac{X_L(\alpha)X_C}{X_L(\alpha)+X_C} = jX_e(\alpha) \quad (1)$$

where:

$$X_L(\alpha) = X_{L0} \frac{\pi}{2(\pi-\alpha)+\sin(2\alpha)} \quad (2)$$

where $\alpha \in \left[\frac{\pi}{2}, \pi\right]$ is the delay angle at the onset of thyristor conduction:

- if $\alpha = \frac{\pi}{2}$ (full conduction), then $X_L(\alpha) = X_{L0} > 0$;
- if $\alpha = \pi$ (thyristors blocked), then $X_L(\alpha) \rightarrow \infty$.

Replacing (2) in (1) yields

$$X_e(\alpha) = X_C \frac{\pi k_X}{\sin 2\alpha - 2\alpha + \alpha} \quad (3)$$

Where:

$$k_X = \frac{X_{L0}}{X_C} \text{ and } \alpha = \pi(2 + k_X) \quad (4)$$

And

$$B_e(\alpha) = -\frac{1}{X_e(\alpha)} = -\frac{\sin 2\alpha - 2\alpha + \alpha}{\pi k_X X_C} = \frac{2\alpha - \alpha - \sin 2\alpha}{\pi k_X X_C} \quad (5)$$

This relation is complemented by the inequality constraints imposed by the admissible range of the delay angle α [5].

$$\left(\frac{\pi}{2} \leq\right) \alpha_{min} \leq \alpha \leq \alpha_{max} (\leq \pi) \quad (6)$$

and

$$B_{emin} = B_e(\alpha_{min}) = \frac{2\alpha_{min} - \sin 2\alpha_{min} - \pi(2+k_X)}{\pi X_{L0}} \quad (7)$$

$$B_{emax} = B_e(\alpha_{max}) = \frac{2\alpha_{max} - \sin 2\alpha_{max} - \pi(2+k_X)}{\pi X_{L0}} \quad (8)$$

When SVC reaches its capability limits it behaves as a fixed compensation device, either reactor or capacitor, depending on the limit reached, with the susceptance values given by eqs. (7) and (8) [7].

These calculation relationships are employed within the steady-state analysis algorithm in the presence of SVCs implemented in the NEPLAN10 software. The software was used to determine the steady-state operating conditions for the scenarios analyzed in the case study.

2.3. Regulator used for dynamic control of the SVC

For the dynamic operation simulations, the CSVGN3-type controller, developed by Siemens/PTI, was employed [10] [11].

The CSVGN3 regulator represents an advanced SVC control model designed to determine the reactive power injected or absorbed by the FACTS device through command of its effective susceptance [12]. The model is grounded in the classical control concept of signal filtering, compensation, and scaling, while additionally incorporating a limiting block based on comparing the control error with a predefined threshold. Fig. 2 illustrates the block diagram of the CSVGN3 regulator [13].

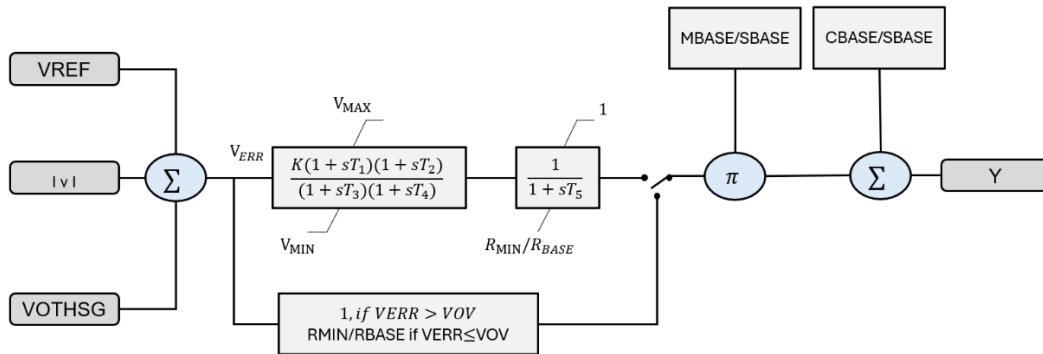


Fig. 2 CSVGN3 regulator diagram

The CSVGN3 controller is typically applied in cases requiring precise and stable SVC performance, providing enhanced protection against excessive control actions under small-signal operating conditions. Through the VOV (Voltage Overdrive) threshold limiter, the controller introduces a dead-zone type response within a specific regulation interval, which is particularly beneficial in systems sensitive to low-amplitude oscillations [14].

The block diagram of the CSVGN3 controller, shown in Fig. 3, consists of the following components:

- Summation block, receiving three input signals: the reference voltage V_{REF} , the measured voltage V , and the auxiliary signal V_{OTHS} (Voltage Othreshold Signal Generator).
- Double lead–lag compensation block, composed of two first-order transfer functions, $(1+sT_1)/(1+sT_2)$ and $(1+sT_3)/(1+sT_4)$, with an overall gain K . The output of this block is limited within the range V_{MIN} to V_{MAX} .
- First-order delay block, represented by the transfer function $1/(1+sT_5)$, to which the compensated signal is subsequently applied.
- Response selection logic, based on the comparison between the error signal V_{ERR} and the overvoltage threshold VOV . If $V_{ERR} > VOV$, the direct controller output is selected; otherwise, a scaled signal is applied.
- Output scaling blocks, M_{BASE}/S_{BASE} followed by C_{BAS}/S_{BASE} , used to obtain the SVC susceptance [15].

Table 1

Parameters adopted for the simulated operating conditions considered in the case study

Parameter	Unit	Description	Value
K	p.u.	Regulator gain	30
T1	s	Filter time constant 1	0.5
T2	s	Filter time constant 2	0.25
T3	s	Compensation time constant 1	0.3
T4	s	Compensation time constant 2	0.02
T5	s	Delay time constant	0.1
VOV	p.u.	Voltage Overdrive	0.1

Table 1 presents the parameter values used in the simulations performed as part of the case study.

3. The test network

The NORDIC32 network developed within the CIGRE Study Committee C4 was chosen because it is a benchmark system for voltage and frequency stability analysis, power oscillation studies, stability analysis methods testing. It has become one of the most used reference models for research and validation of protection/control algorithms [16].

NORDIC32 is a simplified adaptation of an electricity system similar to that of Sweden. A simplified diagram of the 400 kV grid is presented in Fig. 3. The grid is used as a standardized model for the analysis and simulation of power systems. NORDIC32 is made up of 32 nodes, with voltages between 400 kV and 130 kV, interconnected by a system of power lines, power transformers, generators and consumers representing a balanced energy system. The network is divided into four main zones: the northern zone, the southern zone, the central zone, and the equivalent zone. [17]

Depending on the primary source of electricity production and consumption, the four zones can be characterized as follows [18]:

- In the North area, the main source of energy is hydropower plants and consumption is average. The Northern Zone represents the northern part of Sweden and Finland;
- In the southern area, electricity production is based on thermal power plants, this area having a weak connection with the rest of the network;
- Most of the consumers are concentrated in the central area, the main source of generation being the thermal power plants;
- The equivalent area is a simplified energy system that interconnects with the northern area of the grid.

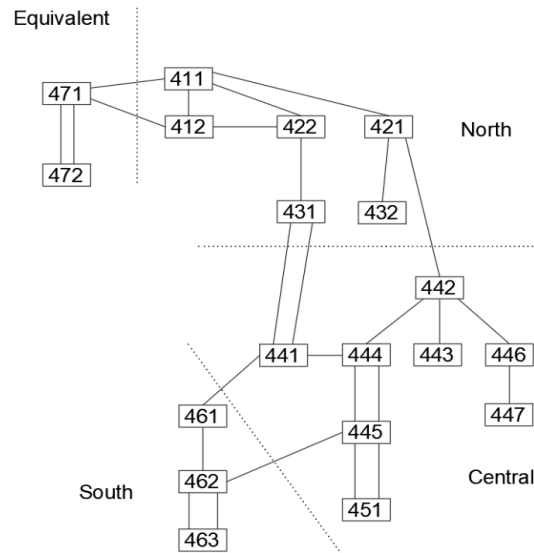


Fig. 3 400 kV nodes in the NORDIC32 network

In the dynamic simulations carried out on the NORDIC 32 test system, the following controllers were used for the control of the generating units in the analyzed area, referred to as the Central area.

AC1A Excitation System

The AC1A excitation system model represents an alternator–rectifier system with uncontrolled rectifiers and voltage regulation achieved through field current feedback. The functional model, control block structure, and parameter set of the AC1A excitation system adopted for the simulation studies fully comply with the model definitions provided in IEEE Std 421.5-2016 [19]. The system employs a separately excited configuration, using diode rectifiers that impose a lower limit on the excitation output voltage [20].

The use of this excitation system model offers the following advantages: a very fast response due to the high level of amplification, accurate voltage regulation achieved through dedicated feedback, and improved stability. [21].

PSS1A Power System Stabilizer

The PSS1A controller is used in the control of generators in thermal power plants to enhance power system stability by damping low-frequency oscillations. The controller has a single input signal, which is typically generator speed, system frequency, or electrical power. The functional representation, control block configuration, and parameterization of the PSS1A power system stabilizer implemented in the simulation studies are in full accordance with the model specifications defined in IEEE Std 421.5-2016 [19].

This type of stabilizer has a simple structure and is widely used in stability studies of large-scale power systems [22].

4. Scenarios analysed within the NORDIC32 network

Scenario 0 represents the normal operating regime of the NORDIC32 test network, in this scenario the electricity production in the central area of the network is exclusively from thermal power plants. In the case study, the focus was on studying the central area where production is deficient compared to very high energy consumption and where energy production is only from thermal power plants [23].

The S1 scenario represents an analysis model for the study of the impact of the energy transition from traditional sources of electricity generation to renewable sources. In this scenario, several high-power classical power plants were disconnected from the central area of the grid and wind power plants distributed in several grid nodes were connected in their place [24]. Compared to the S0 scenario, the following changes have been made as shown in Table 2:

Table 2

Changes to thermal power plants in scenario S1

Power Generation Plant	Power in scenario S0 [MW]	Power in scenario S1 [MW]	Connection node	Energy source type
G15	1080	0	447	Thermal power plant
G16	600	300	451	Thermal power plant
G7	180	0	143	Thermal power plant

Thus, the G15 and G7 generators were completely disconnected from the grid and the power of the G16 generator was reduced by half.

The wind power plants connected in scenario S1 and their connection point are shown in Table 3.

Table 3

Grid-connected wind power plants in the S1 scenario

Power Generation Plant	Power in scenario S0 [MW]	Power in scenario S1 [MW]	Connection node	Energy source type
Wind1	0	360	447	Wind
Wind2	0	360	446	Wind
Wind3	0	100	444	Wind
Wind4	0	150	143	Wind
Wind5	0	170	144	Wind
Wind6	0	300	451	Wind

Scenario 2 is based on grid operation scenario 1, additionally a dimensioned SVC device with a reactive energy compensation capacity of ± 300 MVar is connected to node 444.

5. Analysis of the dynamic operating regime in the studied scenarios

The dynamic event analysed in all three scenarios consists in the occurrence of a fault that leads to the disconnection of the 400 kV line L432-444, this is one of the 400 kV lines that connect the central area and the North area. The disconnection of the line occurs at the moment $t=3$ s [25].

In the context of this event, the time-domain evolution of several network parameters will be assessed for the three investigated scenarios [26]. Specifically, the analysis will focus on the voltage profile at node 444, which represents the terminal node of the feeder and the connection point of the SVC device in Scenario 3. Furthermore, the study will examine the frequency dynamics at node 444, as well as the corresponding rate of change of frequency (ROCOF) at the same location.

The voltage variation in node 444 (VT [pu]) in the three studied scenarios is shown in Fig. 4.

In the S0 scenario, corresponding to the initial system configuration without the integration of renewable energy sources, the disconnection of the 400 kV L432–444 transmission line produces significant transient voltage deviations in node 444. The pre-fault voltage is 0.985 pu. At $t=3$ s, a sharp voltage drop to 0.958 pu occurs, followed by a rebound leading to an overvoltage above 0.975 pu, with well-defined

oscillatory behavior. These oscillations persist until approximately $t=7$ s, after which the voltage converges to a steady-state level of about 0.978 pu.

In scenario S1, where renewable generation is integrated but no Static VAR Compensator (SVC) is connected, the same network event induces a more severe dynamic response. The initial voltage in node 444 is 0.972 pu, lower than in S0. Following the line disconnection at $t=3$ s, the voltage sharply drops to 0.944 pu, triggering oscillations of greater amplitude than those observed in S0. The stabilization process is slower, and the final voltage settles at approximately 0.963 pu, with oscillations persisting in the post-transient regime.

In scenario S2, with both renewable generation and an SVC rated at ± 300 MVar connected to the system, the voltage dynamics are significantly improved. The initial voltage in node 444 is 1.009 pu. At $t=3$ s, a brief voltage dip to 0.984 pu is recorded, followed by a smooth and rapid recovery above 0.995 pu within less than two seconds. From $t=6$ s onwards, the voltage stabilizes precisely at 1.000 pu, with no observable oscillatory components in the steady-state operating condition.

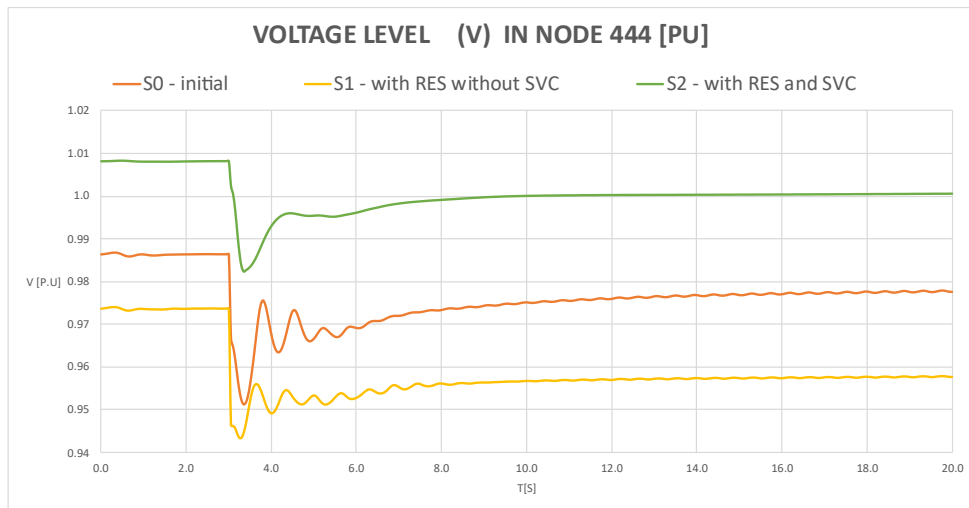


Fig. 4 Voltage at node 444 [pu] in the three scenarios

Table 4 consolidates the results obtained for all three studied scenarios with respect to voltage level variation.

Table 4

Comparative analysis of the case scenarios – voltage variation

Feature	Scenario S0	Scenario S1	Scenario S2
Initial Voltage [pu]	0.985	0.972	1.009
Minimum voltage at $t = 3$ s [pu]	0.958	0.944	0.984
Value stabilized after 15s [pu]	0.978	0.963	1.000

Oscillations	Present, medium	Pronounced, persistent	Absent
Stabilization Time	~ 4 s	~ 5 s	~3 s
Overall stability	Good	Low	Very good

It can be observed from the results presented in Table 4 that in the event of the disconnection of line 432–444, the voltage at node 444 is significantly affected in the absence of a compensation mechanism. The S2 scenario, with SVC in node 444, offers excellent response, with fast stabilization, no oscillations and almost perfectly adjusted voltage.

Fig. 5 illustrates the dynamic relationship between the SVC susceptance (B) and the corresponding reactive power output (Q) expressed in per-unit values. The results highlight the operating behaviour of the SVC under steady-state conditions, transient disturbance, and post-disturbance stabilization.

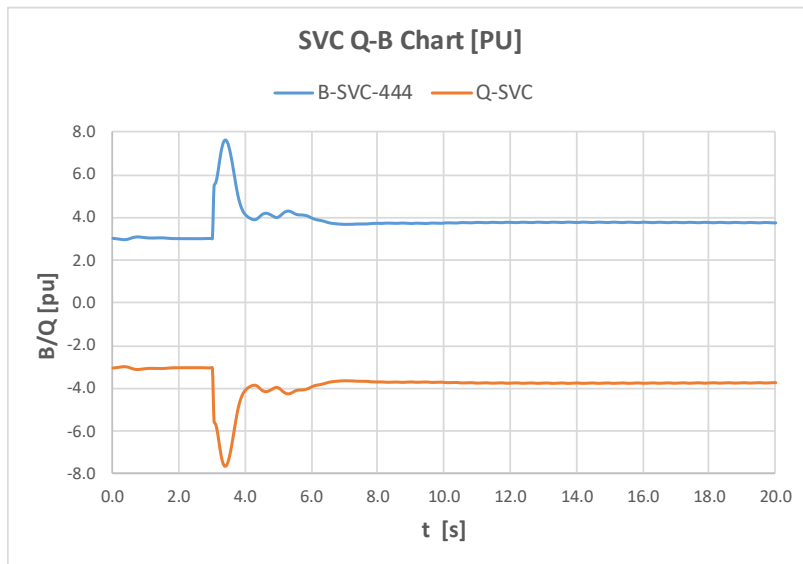


Fig. 5 SVC susceptance (B) - reactive power output (Q) chart

During the initial operating interval, the SVC maintains a nearly constant susceptance, resulting in a stable injection of reactive power. This operating point indicates that the SVC effectively supports the system voltage and operates within its normal regulation range under steady-state conditions.

At $t = 3\text{ s}$, a system disturbance occurs, triggering a rapid adjustment of the SVC susceptance. The controller increases the capacitive susceptance in response to the detected voltage deviation, leading to a corresponding variation in the injected reactive power. This fast response demonstrates the capability of the SVC

to provide immediate voltage support following network perturbations, which is essential for maintaining voltage stability in stressed operating conditions.

Following the initial response, both susceptance and reactive power exhibit damped oscillatory behaviour. These oscillations are associated with the dynamic interaction between the SVC control system and the network. The gradual attenuation of oscillations confirms the dynamic stability of the closed-loop system and indicates adequate damping characteristics.

After the transient period, the SVC reaches a new steady-state operating point characterized by constant susceptance and reactive power output. This final equilibrium reflects the successful restoration of voltage conditions and confirms the effectiveness of the SVC in sustaining reactive power compensation under the new network configuration.

Overall, the susceptance–reactive power characteristics confirm that the SVC operates as intended, providing fast dynamic reactive power support during disturbances and ensuring stable steady-state voltage regulation thereafter. The observed response is consistent with the expected performance of SVC-based voltage control systems in transmission networks.

The rate of change of frequency in node 444 in the three studied scenarios is shown in Fig. 6.

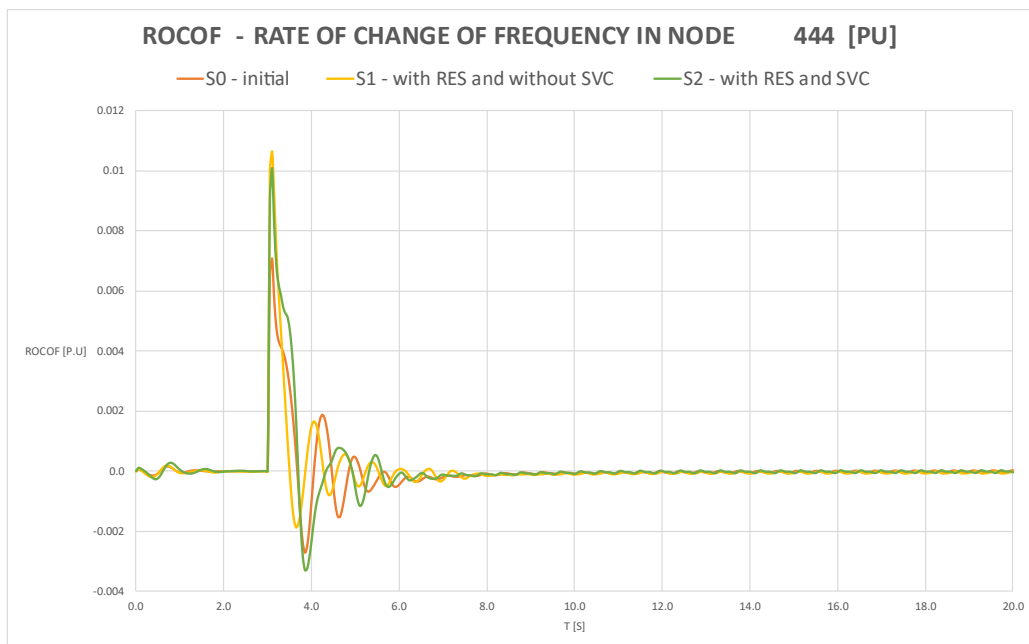


Fig. 6 Rate of change of frequency in node 444 [pu] in the three scenarios

ROCOF is calculated using a discrete differentiation of the system frequency with a sampling interval Δt . The general calculation relationship used is presented below.

$$ROCOF(t) = \frac{df(t)}{dt} = \frac{f(t) - f(t - \Delta t)}{\Delta t} \quad (9)$$

In scenario S0, corresponding to the initial configuration without renewable generation, the Rate of Change of Frequency (ROCOF) exhibits a stable value close to 0.000 pu prior to the disturbance. At $t = 3$ s, a positive peak of +0.0072 pu is recorded, immediately followed by a negative excursion to -0.0029 pu. Subsequently, at $t = 12$ s, a second positive peak of +0.0090 pu occurs, after which the ROCOF reaches a negative minimum of -0.0050 pu. Pronounced oscillations are observed between $t = 3.5$ s and $t = 6.5$ s, after which they are fully damped.

In scenarios S1 and S2 after the power plants are disconnected, the mechanical inertia of the system decreases by 10200 MWs.

In scenario S1, representing the system with renewable sources integrated but without the SVC connected, the ROCOF profile reveals a more severe transient response. The initial positive peak at $t = 3$ s reaches +0.0108 pu—the largest among the three scenarios—followed by a negative oscillation to -0.0033 pu. The ensuing oscillations have greater amplitude and persistence compared to scenario S0, indicating reduced dynamic damping capability.

In scenario S2, where renewable generation operates in conjunction with a ± 300 MVar Static VAr Compensator (SVC), the ROCOF reaches a maximum of +0.0098 pu at the disturbance onset, followed by a negative oscillation to -0.0032 pu. However, the damping is significantly faster in this configuration, with the ROCOF approaching near-zero values and maintaining stability after $t = 5.5$ s.

Table 5

Comparative analysis of the scenarios – ROCOF

Feature	Scenario S0	Scenario S1	Scenario S2
Initial ROCOF [pu]	0.000	0.000	0.000
Positive ROCOF peak at $t = 3$ s [pu]	+0.0072	+0.0108	+0.0098
Post-event negative oscillation [pu]	-0.0029	-0.0033	-0.0032
Stabilization Time [s]	~3	~4	~3
Oscillations	Reduced, short	Pronounced	Moderate
General stability ROCOF	Very good	Good	Very good

The S2 scenario (with SVC) provides the best ROCOF performance under disturbance conditions. Although the initial peak is close to that of the S1, SVC helps to quickly dampen and stabilize the waveform.

Table 6

Scenario/ Parameter	Voltage level	ROCOF
Scenario S0 – base case	It falls within the permissible limits, in the event of a dynamic event or defect, the system stability is good with average oscillations, damped over time.	In the initial scenario, the system response is dynamically stable in the event of an event. The damping time of the oscillations is reduced and their amplitude is limited.
Scenario S1 – with RES	The voltage level varies more in the event of a dynamic event or fault. In terms of variations, these can exceed the maximum allowable limits. Lower dynamic stability compared to the initial scenario	The system response is less stable in scenario S1. The amplitude of oscillations in the event of a fault is larger and the attenuation time is increased.
Scenarios S2 – with RES and SVC	After connecting the SVC device in all dynamic events studied, voltage stability was improved, the level of oscillations decreased and the damping time is much shorter.	Connecting the SVC device produces a small improvement in system response in the event of a dynamic event, but the overall stability of the system remains lower than the initial scenario.

Table 6 presents a summary of the main conclusions obtained from the analyses carried out for the three scenarios studied.

5. Conclusions

The main purpose of this analysis was to identify the challenges faced by electricity transmission grids in terms of dynamic transmission stability in the context of the transition from classical sources of electricity generation to renewable sources. The solution analysed in the case study is represented using SVC devices to increase the dynamic stability of the system and the capacity to integrate renewable sources. The dynamic simulations showed that in the scenario with classical generators the system response is much more stable. This is due to the natural inertia of synchronous machines, their ability to dampen sudden variations in frequency and provide immediate inertial response. In order to increase the operational safety of the network, SVC devices were used. The benefits generated by the integration of FACTS devices at the level of the electricity transmission network identified in the analysed operating regimes are:

- Limitation of voltage drops in nodes immediately affected by the event
- Rapid damping of transient oscillations.
- Return of the voltage to values close to the nominal in a much shorter time compared to the scenarios without SVC.

- Avoidance of excessive overvoltages in case of rapid restoration (e.g. in event 3, where the scenario without SVC generated overvoltages above 1.11 pu).
- By rapidly compensating for reactive imbalances, the SVC stabilizes power flows and supports the voltage profile at critical nodes.
- The maximum deviations were reduced, but significant immediately after SVC contributes to faster damping of frequency oscillations and a smoother trajectory.
- Instantly limit voltage and frequency imbalances.
- It quickly dampens transient oscillations.

In conclusion, through the analysed operating regimes it was found that the integration of renewables is feasible and necessary, but it must be accompanied by a reformulation of control strategies, as well as an adaptation of dynamic simulation methodologies, to correctly reflect the new operational reality of modern electricity systems.

Future work will focus on extending the simulations to additional areas of other transmission networks and on the application of alternative FACTS devices to allow comparative evaluation of the results.

REFERENCES

- [1] CIGRE Study Committee B4 - "Static VAr compensator/statcom performance survey results – 2017 and 2019";
- [2] C. Constantin, M. Eremia, I. C. Constantin, and L. Toma, "Application of shunt FACTS devices for a secure and efficient operation of the Romanian power system," *UPB Sci. Bull. Ser. C Electr. Eng. Comput. Sci.*, vol. 76, no. 4;
- [3] P. Kundur, M. Klein, G. J. Rogers, and M. S. Zywno, "Application of power system stabilizers for enhancement of overall system stability," *IEEE Transactions on Power Systems*, vol. 4, no. 2, pp. 614–626, May 1989;
- [4] C. M. Ifeanyi, O. Gregory, and C. Linus, "Improving Constant Power Supply in Renewable Energy Integration and Optimization Using ANN-Based SVC," *American Journal of Multidisciplinary Research and Innovation*, vol. 4, no. 3, pp. 205–215, 2025, doi: 10.54536/ajmri.v4i3.4821;
- [5] M. Eremia, M. Sănduleac, L. Toma, C. Bulac- " FACTS devices Concepts an applications in power systems," Ed. AGIR, 2017;
- [6] IEEE 1031-2011 – "Guide for the Functional Specification of Transmission Static Var Compensators";
- [7] M.Eremia "Electric Power Systems – Electric Networks," Romanian Academy Publishing House, 2006;
- [8] N. G. Hingorani and L. Gyugyi, *Flexible AC Transmission Systems (FACTS)*, IEEE Press / John Wiley & Sons, Hoboken, NJ, USA, 2019;
- [9] M. Young, *The Technical Writer's Handbook*. Mill Valley, CA: University Science, 1989;
- [10] Siemens Power Technologies International, *PSSE Model Library: Static VAr Compensator (CSVGNx Voltage Regulator Models)*, Siemens PTI, Schenectady, NY, USA, Technical Documentation;

- [11] A. J. Wood, B. F. Wollenberg, and G. B. Sheblé, *Power Generation, Operation, and Control*, John Wiley & Sons, Hoboken, NJ, USA, 2013;
- [12] CIGRÉ Study Committee B4, *Static VAR Compensators—Application and Benchmark Models*, CIGRÉ Technical Brochure No. 229, Paris, France, 2003. ISBN: 978-2858738912;
- [13] R. Adapa, "High-Performance Static VAR Compensators for System Dynamic Performance," *IEEE Computer Applications in Power*, vol. 7, no. 1, pp. 38–43, Jan. 1994. doi: 10.1109/67.259770.
- [14] F. Alsalem and A. Z. Faza, "Static VAR Compensator Control Using Phasor Measurement Unit Feedback Signals for Voltage Stability Improvement in Power Systems," *Energy Science & Engineering*, vol. 13, no. 7, pp. 3569–3587, Apr. 2025, doi: 10.1002/ese3.70114.
- [15] K. M. Berdugo Sarmiento, J. I. Silva-Ortega, V. Sousa Santos, J. E. Candelo-Becerra, and F. E. Hoyos, "Improving the Operation of Transmission Systems Based on Static VAR Compensator," *Electricity*, vol. 6, no. 3, art. 40, 2025, doi: 10.3390/electricity6030040.
- [16] T. Van Cutsem and Lampros Papangelis, "Description, Modeling and Simulation Results of a Test System for Voltage Stability Analysis"
- [17] D. Peppas, V. Knazkins and M. Ghandhari, "Development and Analysis of Nordic32 Power System Model in PowerFactory,"
- [18] T. Van Cutsem, et al., "Test Systems for Voltage Stability Studies," *IEEE PES Task Force Report*, Tech. Rep., 2010.
- [19] IEEE, *IEEE Std 421.5-2016 – IEEE Recommended Practice for Excitation System Models for Power System Stability Studies*, IEEE Power & Energy Society, New York, USA, 2016.
- [20] A. S. Abdel Moamen and M. A. El-Sharkawy, "Optimal tuning of power system stabilizers and excitation system parameters," *Electric Power Systems Research*, vol. 71, no. 1, pp. 1-9, Oct. 2004. doi: 10.1016/j.epsr.2004.01.004.
- [21] R. A. Ramos, N. G. Bretas, and L. C. P. da Silva, "A new methodology for the coordinated tuning of AVR and PSS controllers in multimachine power systems," *IEEE Transactions on Power Systems*, vol. 21, no. 4, pp. 1878-1887, Nov. 2006. doi: 10.1109/TPWRS.2006.883678.
- [22] I. Kamwa, R. Grondin, and Y. Hebert, "Wide-area measurement based stabilizing control of large power systems—A PSS1A case study," *IEEE Transactions on Power Systems*, vol. 14, no. 3, pp. 1164–1171, Aug. 1999. doi: 10.1109/59.780902.
- [23] A. T. Alemu and G. M. Meseret, "Optimal Location and Sizing of Static VAR Compensator (SVC) to Improve Voltage Profile in Distribution Network," *Engineering Reports*, vol. 7, no. 10, Oct. 2025, doi: 10.1002/eng2.70435.
- [24] C. Norlander et al., *The Impact of Offshore Wind Power Hybrid AC/DC Connections on System Operations and System Design*, CIGRE Technical Brochure 972, 2025.
- [25] Murtadha Sami, Stefan Gheorghe, Lucian Toma - "Voltage security improvement in transmission networks using SVC device," in *Scientific Bulletin of the University Politehnica of Bucharest 2022*
- [26] M. Chouki, H. Belila, and H. Zaimen, "Study of Flexible AC Transmission Systems and Static VAR Compensator and Their Behavior on Power and Voltage Control in Transmission Networks," *Mathematical Modelling of Engineering Problems*, vol. 12, no. 7, 2025, doi: 10.18280/mmep.120729.